# Review of Power Control in Research Reactor

Im Yun-Taek[a*], Doo Seung-Gyu[a]  and Kim Ki-Hyun[a]
*[a] Korea Atomic Energy Research Institute, 989-111 Daedeok-daero, Yuseong-gu, Daejeon 34057, Korea.*
*HANARO Management Division.*
*[*]Corresponding author: ytim@kaeri.re.kr*

## 1. Introduction

HANARO is a pool-type reactor that has a power capacity of 30MWth. It has been successfully operated for over 20 years, and functional algorithms of the computer control system have been proved for safe control of power demand.

The purpose of this work is to offer and review a fundamental design approach of a research reactor control system to be applicable to other plant control systems. The control technique described in this paper is based on the HANARO control system.

## 2. Design Considerations

### 2.1 Delayed Response Model

Relative to the neutron power response, the thermal power response much more slowly reaches steady state due to time delays of the hydraulic system. Analysis of the actual system should be performed in consideration of a distributed network, as shown in Fig. 1, but such an approach may be too complicated to be applicable to system implementation [1]. The time delay model of heat transfer is generally expressed as an exponentially attenuating function [2], and Fig. 2 shows the whole function block of the control system including the time delay model. Laplace transforms of the two delayed loops can be simply expressed as Equation-(1).

$$\frac{N_1(s)}{N_0(s)}\frac{N_2(s)}{N_1(s)} = \frac{1}{(1+sT_1)}\frac{1}{(1+sT_2)} \tag{1}$$

Thus, the time domain analysis is now written as Equations (2-a) and (2-b) for digital signal processing.

$$N_1\big(T_S(k+1)\big) = e^{-T_S/T_1}N_1(T_Sk) + (1-e^{-T_S/T_1})N_0(T_Sk) \tag{2-a}$$

$$N_2\big(T_S(k+1)\big) = e^{-T_S/T_2}N_2(T_Sk) + (1-e^{-T_S/T_2})N_1(T_Sk) \tag{2-b}$$

It should be noted that this interpretation is based on a simple heat transfer model of a heating system [2]. However, an extra hydraulic model can be added as necessary, since heat transfer in the distributed network can partially occur, as shown in Fig. 1.

The time constants $T_1$ and $T_2$ in Fig. 2 are the delay times to reach steady state in the primary and the secondary systems, and these constants are proportional to the total volume of coolant, but inversely proportional to the flow rate of the coolant [1]. $T_S$ is the sampling interval of the system.

Further, the extra time constant is added to the response time and $K_2$ is the additional low pass filter response. In an ideal case, $K_3$ is equal to 1. Otherwise, $K_3$ will keep track of the thermal-to-neutron power ratio.

When it is necessary to ignore such time delays caused by the heat transfer process, $K_3$ can be simply set to 1.

### 2.2 Optimal Switching Point

The measurement range of a NMS (Neutron Monitoring System) generally covers over ten decades [3], and it is so wide that the NMS uses log power and linear power. The log power covers a wide range and provides better power resolution than the linear power resolution in low-power mode operation. On the other hand, the linear power resolution is better than the log power resolution in high-power mode. Therefore, to accurately control the reactor power, the optimal transition point of the neutron level should be decided.

The resolutions of the log and linear power in the control computer system can be expressed by Equations (3-a) and (3-b).

$$\Delta N_{linear} = \frac{N_{max} - N_{min}}{2^{16bit} \times (4/5)} \tag{3-a}$$

$$\Delta N_{log} = \frac{\log_{10}(N_{max}) - \log_{10}(N_{min})}{2^{16bit} \times (4/5)} \tag{3-b}$$

$N_{max}$ and $N_{min}$ are the maximum and minimum of the neutron power, respectively. It is assumed that a NMS (Neutron Monitoring System) transmits 4~20 [mA] (or 1~5 [V] with 250 [ohm] in the receiver), and receivers in the control computer use 16-bit ADCs.

Obviously, the optimal switching point can be found where the resolution of the log power is equal to the increment of the log power, as in Equation-(4).

$$\Delta N_{log} = \log_{10}(N + \Delta N_{linear}) - \log_{10}(N) \tag{4}$$

Rewriting Equation-(4), the switching point can be found using Equation-(5) with respect to $N$.

$$N = \Delta N_{linear}/\big(10^{\Delta N_{log}} - 1\big) \tag{5}$$

For example, if $N_{max}$ and $N_{min}$ are 150 %FP (Full Power) and $10^{-8}$ %FP, then the point is about 6.4 %FP, found by Equation-(5). The control computer can use two switching points (6.4 and 6.9 %FP) to avoid an oscillatory behavior at the transition of the mode.

### 2.3 Anti-Windup

The purpose of an anti-windup is to provide local feedback to make the control system stable when the loop is saturated; the effect of the anti-windup is to reduce both overshoot and control effort in the feedback system [4]. To implement anti-windup techniques, a saturation element is used to limit the output value. $K_1$, $K_3$, $V_1$, and $V_2$ are limited output signals of the anti-windup technique, as shown in Fig. 2.

The output of the logarithm function multiplied by $G_1$ is from -1 to +1 for the anti-windup. Strictly speaking, the logarithm function is not a saturation element. However, it acts like a saturation element when the input is suddenly increased. On the other hand, it functions almost linearly when the input is close to 1. Equation-(6) is the Taylor series representation of the logarithm when $x$ is small ($|x|<1$).

$$\log_{10}(1+x) \approx \frac{x}{\ln(10)} \qquad (6)$$

Thus, when the ratio of PDM-to-Power (*Error*) is small enough to be represented as a Taylor series, the error varies almost linearly.

### 2.4 Control Rod Movement

The value $V_1$ is a parameter determined by the error and the log-rate ($N_{lograte}$), as shown in Fig. 2, and is used to move the control rods. The gains $G_1$ and $G_2$ have an influence on the rod movement, and separating the first and second terms in Equation–(7) provides rough estimations of the gains.

$$V_1 = \left| G_1 \log_{10}(Error) \right|_{-1}^{+1} - G_2 N_{lograte} \Big|_{-1}^{+1} \qquad (7)$$

For example, if PDM (Power Demand) is increased up to 120 % versus the present power level, then $G_1$ can be set at 12.63 ($1/\log_{10}(1.2/1)$) regardless of the second term. This means that the control rod will move up maximally when PDM is larger than 120%. If $G_2$ is set at 0.2, then the control computer will stop moving the control rod at the log-rate of over 5%/Sec, regardless of the first term. This means that the permissible maximum log-rate is 5%/Sec. Otherwise, the control rod moves to decrease the power over 5%/Sec since the maximum value of the first term is 1 [5].

### 2.5 Compensation

To improve the dynamic behavior of the control system, a lag compensator is used. The action of the lag compensator is similar to that of a PI controller, which increases the low-frequency gain and improves steady state accuracy. Therefore, the response will be slower. Since the positons of two corner frequencies ($G_4/T_4$ and $1/T_4$) affect the low-frequency gain ($G_4$) [4], these frequencies can be chosen in accordance with the plant variables under assumption that no aliasing occurs.

Equation-(8) is the difference equation for the lag compensator for digital signal processing, as shown in Fig. 1.

$$V_2(T_s(k+1)) = \left| a \bullet V_2(T_s k) + b \bullet V_1(T_s(k+1)) + c \bullet V_1(T_s k) \right|_{-1}^{+1} \qquad (8)$$

The constants a, b, and c depend on IIR filter design techniques. The implementation of this digital filter is commonly achieved by approximation of derivatives, or by the bilinear transformation called Tustin's method [6].

Although $V_1$ varies within a limited range ($|V_1|\leq1$), its range is further reduced due to the low-frequency gain of the compensator ($|V_1|<(1/G_4)$). Thus, the effective range of $V_1$ is approximated as $|V_1|\leq0.2$ when the low-

frequency gain ($G_4$) of the compensator is 5. Accordingly, if the control rod is assumed to move up maximally, then $N_{lograte}$ will be 4 %/Sec at most ($0.2=1-0.2\times N_{lograte}$) by Equation-(7).

Finally, the number of steps ($V_3$) is transformed to binary data to drive the step motor drivers, as in Equation-(9), where $G_3$ is the maximum step number.

$$V_3 = Unit(G_3 \times V_2) \qquad (9)$$

### 2.6 Thermal Power

The actual thermal power, when the reactor is providing enough heat to allow calorimetric measurement, is proportional to the flow rate and temperature difference between the inlet and the outlet of the heat exchanger in the secondary cooling system as Equation-(10) [7].

$$Q_{SCS} = C \times FR_{SCS} \times \Delta T_{SCS} \qquad (10)$$

The constant $C$ is the specific heat of the coolant; $FR_{SCS}$ and $\Delta T_{SCS}$ (or $T_A$-$T_B$) are shown in Fig. 1. However, if the measured thermal power includes other heat sources, then the net thermal power is recalculated after leaving out the pumps contribution ($Q_{Pump}$) and the thermal power absorbed by the pool ($Q_{Bypass}$), as in Equation-(11).

$$Q_{Net} = Q_{SCS} - Q_{Pump} - Q_{Bypass} \qquad (11)$$

### 3. Conclusions

Control techniques of a research reactor were reviewed based on HANARO. The heat transfer model of a hydraulic system is similar to that of the heating system. To control a wide range of the neutron level, a logarithmic signal is used, and the optimal switching point between the log power and the linear power is calculated. To avoid excessive responses, an anti-windup technique is used with saturation elements. A lag compensator, similar to a PI controller, is used to improve the steady-state accuracy. The net thermal power is calculated by calorimetric measurement.

### REFERENCES

[1] M. A. Schultz. "*Control of Nuclear Reactors and Power Plants*", McGraw-Hill. 1955.
[2] Katsuhiko Ogata, "*System Dynamics 3rd*", Prentices Hall, 1998.
[3] Böck, H. and Villa, M., 2004, "TRIGA Reactor Main Systems", IAEA Number: AIAU 24311, May 2004.
[4] Gene F. Franklin et al., "*Feedback Control of Dynamic Systems 4th*", Prentice Hall, 2002.
[5] Dane Bang *et al*, "*Feedback Power Control for TRIGA-II Research Reactor*", KNS Jeju, 2017. May 18-19.
[6] John G. Proakis, "*Digital Signal Processing 3rd*", Prentice Hall. 1996.
[7] Yunus. A. Cengel, "*Heat Transfer 2nd: A Practical approach*", chapter 13, McGraw-Hill, 2002.
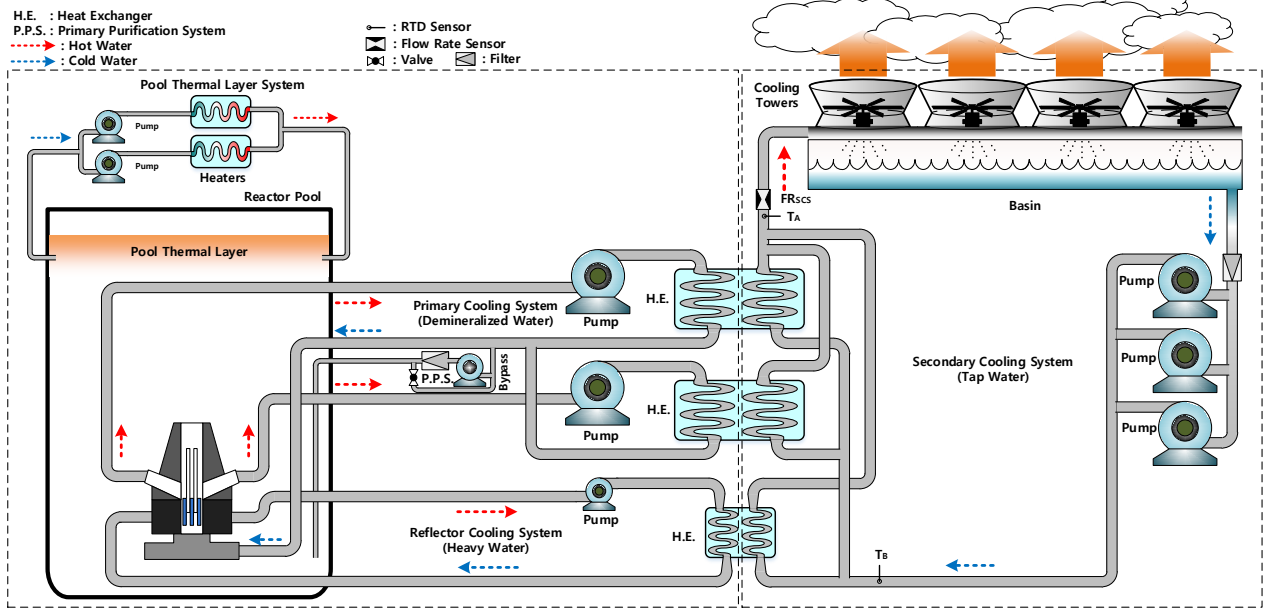
Fi g. 1. Schematic diagram of heat transfer during operation of HANARO.
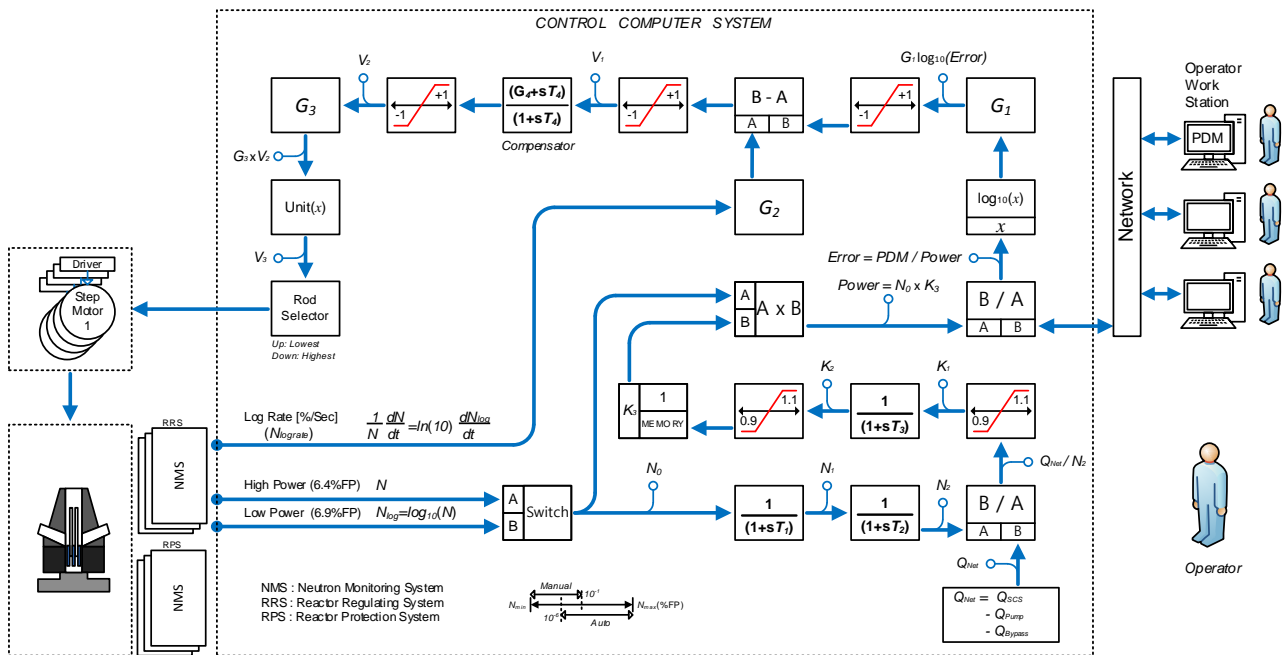


Fi g. 2. Functional block diagram of control computer system